Probing potassium channel function in vivo by intracellular delivery of antibodies in a rat model of retinal neurodegeneration

Dorit Raz-Prag[a,1], William N. Grimes[b], Robert N. Fariss[c], Camasamudram Vijayasarathy[a], Maria M. Campos[c], Ronald A. Bush[a], Jeffrey S. Diamond[b], and Paul A. Sieving[a,d,2]

[a]Section for Translational Research in Retinal and Macular Degeneration, National Institute on Deafness and Other Communication Disorders, [b]Synaptic Physiology Section, National Institute of Neurological Disorders and Stroke, and [c]Biological Imaging Core Facility, [d]National Eye Institute, National Institutes of Health, Bethesda, MD 20892

Inward rectifying potassium (Kir) channels participate in regulating potassium concentration (K$^+$) in the central nervous system (CNS), including in the retina. We explored the contribution of Kir channels to retinal function by delivering Kir antibodies (Kir-Abs) into the rat eye in vivo to interrupt channel activity. Kir-Abs were coupled to a peptide carrier to reach intracellular epitopes. Functional effects were evaluated by recording the scotopic threshold response (STR) and photopic negative response (PhNR) of the electroretinogram (ERG) noninvasively with an electrode on the cornea to determine activity of the rod and cone pathways, respectively. Intravitreal delivery of Kir2.1-Ab coupled to the peptide carrier diminished these ERG responses equivalent to dimming the stimulus 10- to 100-fold. Immunohistochemistry (IHC) showed Kir2.1 immunostaining of retinal bipolar cells (BCs) matching the labeling pattern obtained with conventional IHC of applying Kir2.1-Ab to fixed retinal sections postmortem. Whole-cell voltage-clamp BC recordings in rat acute retinal slices showed suppression of barium-sensitive Kir2.1 currents upon inclusion of Kir2.1-Ab in the patch pipette. The in vivo functional and structural results implicate a contribution of Kir2.1 channel activity in these electronegative ERG potentials. Studies with Kir4.1-Ab administered in vivo also suppressed the ERG components and showed immunostaining of Müller cells. The strategy of administering Kir antibodies in vivo, coupled to a peptide carrier to facilitate intracellular delivery, identifies roles for Kir2.1 and Kir4.1 in ERG components arising in the proximal retina and suggests this approach could be of further value in research.

Kir | peptide carrier | Pep-1 | retinal bipolar cells | Müller cells

Inward rectifying potassium (Kir) channels are well represented in the CNS and the retina (1). Kir subfamilies share amino acid homology but differ in mode of activation or degree of rectification (2, 3). Histological evidence of clustering of Kir4.1 channels on Müller glial cell proximal endfeet adjacent to the vitreous (4–6) and electrophysiological data (7–9) implicates Kir4.1 in "potassium siphoning" in the proximal mammalian retina (10–12). Members of Kir subfamilies are also reported on retinal neurons in the inner-nuclear (INL) and inner-plexiform (IPL) layers (13). Strongly inward rectifying Kir2.1 is ubiquitous in neurons in the central nervous system (14–16); however, Kir2.1 localization in the retina remains ambiguous as it is reported alternatively on Müller cells (17, 18) or on neurons (13, 19). The role of Kir2.1 in ERG response generation has not been explored.

Light-induced increases in extracellular potassium (K$^+$) in the proximal retina contribute to electroretinogram (ERG) potentials (7), including the scotopic threshold response (STR), a small negative-going wave elicited by extremely dim stimuli near rod threshold (7, 20, 21). The photopic negative response (PhNR) is similar to the STR in polarity and timing but is recorded under light-adapted conditions (22). Intraretinal recordings (8) suggest that potassium fluxes in the proximal retina contribute to cornea-negative responses in the photopic ERG, homologous to the STR. The STR and PhNR amplitudes are considerably enhanced and easily recorded from the dystrophic Royal College of Surgeons (RCS) rat (23, 24), which carries a homozygous *Mertk* deletion mutation (25) causing slowly progressive outer retinal degeneration (26, 27) that subsequently also involves proximal retinal structures (28, 29). Building on these observations, we probed Kir channel function in the retina of RCS rat in vivo. As patch recordings with barium (Ba^{2+}) have identified strongly rectifying Kir channels on isolated cone bipolar cells (BCs) (30), we initially tried intravitreal injections of Ba^{2+} and observed reduced ERG components consistent with reports (7, 8, 31, 32). However, Ba^{2+} blocks Kir channels nonselectively and does not distinguish activity of channel subtypes. Because drugs that suppress specific Kir channel subtypes are not available, we explored use of Kir-Ab. The Kir-Ab epitopes are on the C-terminal domain within the cell, and we coupled the Kir-Abs to an amphipathic peptide carrier to facilitate delivery across retinal cell membranes to reach intracellular targets. We found that intravitreal injection of the Kir-Ab:carrier complex in vivo suppressed the retinal ERG function, and immunohistochemistry (IHC) showed that the Kir-Ab had reached specific cellular targets that we characterized separately by conventional IHC postmortem immunolabeling of fixed retinal sections.

Results

Kir2.1 Immunolocalization in the RCS Rat Retina. We identified Kir2.1 channels using IHC in two ways. First, we used the conventional method of applying antibody postmortem to fixed tissue. Alternatively, we delivered antibodies in vivo by intravitreal injection. Conventional IHC localized the Kir2.1-Ab to synaptic terminals in IPL sublamina 5, identified as rod and cone BC terminals by colabeling with PKCα and PKCβ, respectively (Fig. 1A and C and Kir-Ab specificity indicated in Fig. S1). This concurs with previous reports of Kir2.1 on neurons in proximal retina (17, 18). Colabeling with VGLUT1 provided additional evidence that Kir2.1 localized to BCs (Fig. S2A). As PKCα labels some amacrine cells in rat (33, 34), we marked amacrine cell termini with

NEUROSCIENCE

Fig. 1. Immunohistochemical colocalization of Kir2.1 with rod and cone BC markers. (*A*) Conventional postmortem double labeling of retinal sections with Kir2.1-Ab (red) and PKCα-Ab (green) in a congenic nondystrophic RCS rat shows colocalization with rod BC termini. (*B*) In vivo intravitreal application of Kir2.1-Ab:carrier (red) in 9-wk-old dystrophic RCS rat followed by double labeling postmortem with PKCα-Ab (green) shows colocalization at rod BC termini. (*C*) Conventional postmortem double labeling of retinal sections with Kir2.1-Ab (red) and PKCβ-Ab (green) in a congenic nondystrophic RCS rat shows colocalization at cone BC termini. (*D*) In vivo intravitreal application of Kir2.1-Ab:carrier (red) in 9-wk-old dystrophic RCS rat followed by double labeling postmortem with PKCβ-Ab (green) shows colocalization at cone BC termini. GCL, ganglion cell layer; IPL, inner plexiform layer; INL, inner nuclear layer; ONL, outer nuclear layer. *Insets* show higher magnification of areas indicated with rectangle (likewise in all IHC figures).

synapsin I/II (35) and found that Kir2.1-Ab labeled synapse elements adjacent to the synapsin-labeled structures rather than directly colocalizing with synapsin I/II (Fig. S2*B*), consistent with Kir2.1 at the rod BC termini (36). Although Kir2.1 channels were reported along Müller cell membranes using the same antibody we used (18), in our hands the Kir2.1-Ab did not colocalize with the Müller cell GFAP marker by conventional postmortem double labeling in RCS rat (Fig. S2*C*).

We also explored whether we could deliver antibody in vivo to the proper intracellular targets. Kir2.1-Ab was coupled to the peptide carrier and delivered by intravitreal injection, after which animals were killed and the immunostaining pattern was observed. This in vivo method showed that Kir2.1-Ab labeled BC terminals, identified by PKCα and PKCβ antibodies applied to the fixed sections postmortem (Figs. 1 *B* and *D*). Of 12 eyes injected with Kir2.1-Ab:carrier complex, 10 eyes showed the pattern of Kir2.1 labeling on rod and cone BCs as we had seen previously by conventional IHC postmortem labeling. Kir2.1-Ab in vivo also sometimes labeled ganglion cell and INL structures, as others reported (13, 19) and distal IPL formations that colocalized only partially with the BC markers. This pattern was inconsistent between eyes and did not correlate with the conventional labeling postmortem. It likely represents nonspecific antibody labeling or antibody entering the cells in vivo but not specifically bound to antigen and then trapped there when the tissue was fixed. Similar indiscriminate and nonspecific labeling of retinal cells was observed in the control eyes following IgG:carrier application (Fig. S3).

In Vivo Application of Kir2.1-Ab Suppresses ERG Activity. In preliminary studies, intravitreal injection of naked antibody alone did

Fig. 2. Functional effect of in vivo delivery of Kir2.1-Ab:carrier on STR and PhNR electronegative ERG potentials. (*A*) Intravitreal application of antibody alone (red trace, *Left* IHC panel) did not alter ERG responses and showed no specific IHC labeling. Black trace and *Right* IHC panel are of the contralateral control IgG injected eye. Shown are the light-adapted responses at 0.6 log cd-s/m² stimulus intensity in a 14-wk-old dystrophic RCS rat. (*B*) Intravitreal application of Kir2.1-Ab:carrier in a 12-wk-old dystrophic RCS rat suppressed the electronegative ERG components. Dark- and light-adapted ERG responses of eyes receiving the Kir2.1-Ab:carrier complex (red traces) show reduction of STR and PhNR amplitudes, respectively, compared with the responses of the contralateral eye injected with IgG:carrier (black). The STR amplitude of the eye injected with Kir2.1-Ab:carrier for a stimulus of −2.4 cd-s/m² is comparable to that of the contralateral control eye for −4.4 cd-s/m² (marked with a double-headed arrow), indicating suppression of retinal function equivalent to dimming the stimulus 100-fold. Responses within the ellipse indicate the emergence of the b-wave. As brighter stimuli ≥ −2.4 log cd-s/m² were required to elicit dark-adapted b-wave responses, the STR could be measured in relative isolation from other ERG components. The PhNR amplitude at 0.1 log cd-s/m² for the Kir2.1-Ab:carrier eye was comparable to the response at −0.9 log cd-s/m², or 10 times dimmer, for the contralateral IgG:carrier eye.

not show appreciable ERG effects (Fig. 2*A*). The experimental strategy became successful once the antibody was coupled with the carrier peptide. Figure 2*B* shows the baseline ERG of a 12-wk-old RCS dystrophic animal, which characteristically lacks scotopic b-wave responses except for a small remnant elicited with brighter stimuli (23). The photopic b-wave under light-adapted conditions is also considerably reduced (24), and the ERG response is pri-

marily an overly large cornea-negative photopic PhNR component. Others have observed that residual signaling by degenerating photoreceptors still yields considerable proximal retinal neuronal activity and K^+ increase in the RCS dystrophic rat (37).

Within 2 h after intravitreal in vivo application of the Kir2.1-Ab:carrier complex, the STR and PhNR amplitudes were diminished compared with contralateral fellow eyes injected with rabbit IgG:carrier (Fig. 2B). Rats were sacrificed after the ERG recordings, and the retinal immunostaining pattern was evaluated. The inclusion criterion for the ERG experiments was successful bilateral in vivo antibody administration. Of the 10 animals successfully injected in vivo with Kir2.1-Ab:carrier that showed IHC labeling equivalent to conventional postmortem Kir2.1-Ab labeling in separate control animals, 5 also showed successful IgG:carrier labeling in the contralateral eyes by IHC and were included in the ERG analysis. The STR amplitude elicited with -3.4 log cd-s/m^2 stimuli was reduced nearly by half (47 ± 10%, mean ± SE, $n = 5$) relative to the respective IgG:carrier contralateral control eyes. STR suppression by Kir2.1-Ab was equivalent to reducing the stimulus intensity ≈2-log units compared with the contralateral IgG:carrier eye (Fig. 2B). The pres-

ent structural and functional findings indicate a role for Kir2.1 channels in the STR response, either directly through BC handling of potassium fluxes or indirectly through BC synaptic input to amacrine cells in the rod pathway. Under light-adapted conditions, application of Kir2.1-Ab:carrier in vivo reduced the PhNR in these animals by 26 ± 8% ($n = 5$) for 0.6 log cd-s/m^2 stimuli, equivalent to reducing the stimulus by 1-log unit (Fig. 2B) and implicating Kir2.1 activity in electronegative ERG responses of the cone pathway through the proximal retina.

Whole-Cell BC Response to Kir2.1-Ab in Retinal Slice. Effects of Kir2.1-Ab on individual BP cells were evaluated by whole cell voltage-clamp recordings from morphologically identified rod and cone BCs in acute retinal slices with the inclusion of Kir2.1-Ab, IgG, or no additional reagent in the patch pipette. Ba^{2+} potently blocks Kir currents in isolated Müller cells from tiger salamander (38) and isolated cone BCs from rat (18). Consistent with previous reports, families of hyperpolarizing voltage steps (from -60 to -140 mV in 20-mV increments for 200 ms) elicited inwardly rectifying currents that were sensitive to 100 μM Ba^{2+} in both cone and rod BCs (Fig. 3 C and D Left) when using control

Fig. 3. Intracelluar Kir2.1-Ab reduces Kir currents in BC whole-cell voltage clamp recordings. Including Kir2.1-Ab in the intracellular solution during whole-cell BC recordings reduces Ba^{2+}-sensitive Kir current. (A and B) Two-photon 3D reconstruction of a cone BC (A) and rod BC (B) filled through the patch pipette with 20 μM AlexaFlour 488. The fluorescence image is superimposed upon a transmitted IR-differential interference contrast (DIC) image of a single focal plane. (C and D) $Ba^2$$^+$-sensitive currents from a typical cone BC (C) and rod BC (D). (Left) Current–voltage relation of response to 200 ms voltage steps from -60 mV to a series of hyperpolarized potentials in control solution (black) and in the presence of 100 μM Ba^{2+} (gray). (Right) Typical current traces for voltage steps to -140 mV in control solution (black) and in the presence of Ba^{2+} (gray). (E and F) Summary ($n = 6$ in all cases) of Ba^{2+}-sensitive current amplitude (voltage steps from -60 to -140 mV) when the intracellular solution contained the Kir2.1-Ab (32 ng/μL; gray), IgG (32 ng/μL; white) or no additional reagent (control; black). Paired (to examine Ba^{2+} sensitivity within groups; in parentheses) and unpaired (to compare Ba^{2+} sensitivity between groups) two-tailed t tests of significance (*P <0.05, **P <0.01, ***P < 0.001).

Fig. 4. IHC of rat retina shows Kir4.1 colocalization with Müller cell GFAP marker. (*A*) Conventional postmortem double labeling with Kir4.1-Ab (red) and GFAP-Ab (green) shows colocalization with Müller cells in a dystrophic 14 wk-old RCS retina. (*B*) In vivo intravitreal application of Kir4.1-Ab:carrier complex gives prominent labeling of Müller cell endfeet with extensions along Müller cell processes in the IPL (red) in a 15-wk-old dystrophic RCS rat and colocalizes with GFAP (green). GCL, ganglion cell layer; IPL, inner plexiform layer; INL, inner nuclear layer; ONL, outer nuclear layer.

patch electrode solution. Inwardly rectifying potassium currents were quantified by measuring the Ba^{2+}-sensitive current in response to voltage steps to -140 mV (measured by averaging 50 ms of the current trace starting at 100 ms after the onset of the voltage step; Fig. 3 *C* and *D Right*). Significant Ba^{2+}-sensitive currents were observed in cone BCs (Fig. 3*E*) dialyzed with control patch solution (12 ± 6 pA (mean $\pm$ SD); $P = 0.005$; $n = 6$) and patch solution containing IgG (10 ± 3 pA; $P = 0.0002$; $n = 6$), but not when patch solution containing Kir2.1-Ab was used (1 ± 7 pA; $P = 0.67$; $n = 6$). Kir channel-mediated currents in control or IgG-filled cone BCs were significantly larger than those recorded in cells filled with Kir2.1-Ab ($P = 0.018$ and $P = 0.02$, respectively). These results indicate that cone BCs express a functional population of Kir2.1. Although the effect was more variable in rod BCs (Fig. 3*F*), Ba^{2+} blocked a significant amount of current in control (13 ± 12 pA; $P = 0.0499$; $n = 6$) and in the presence of intracellular IgG (13 ± 12 pA; $P = 0.042$; $n = 6$), but not in the presence of intracellular Kir2.1-Ab (6 ± 10 pA; $P = 0.17$; $n = 6$). Unpaired comparisons between control or IgG and Kir2.1-Ab rod BC groups did not reach statistical significance ($P = 0.36$ and $P = 0.32$, respectively; Fig. 3*F*), suggesting that rod BCs variably express functional Kir2.1 channels, possibly in addition to other Kir subtypes.

Kir4.1-Ab:Carrier Application in Vivo. We repeated the in vivo ERG and IHC studies using Kir4.1-Ab:carrier complex (Alomone Labs) and observed labeling of Müller cell endfeet and soma (Fig. 4), consistent with our conventional IHC postmortem labeling and with literature reports (18). Of 22 eyes injected with Kir4.1-Ab:carrier, 12 eyes showed successful Kir4.1 labeling of the expected target cell. In ERGs done (before sacrifice) on animals with successful application of the Kir4.1-Ab:carrier and simultaneous successful application of IgG:carrier to the contralateral eye, the PhNR was reduced by $28 \pm 8\%$ ($n = 8$; stimulus intensity 0.6 log cd-s/m^2) relative to the respective contralateral control eye, and the STR was reduced by $33 \pm 9\%$ ($n = 5$; stimulus intensity -3.4 log cd-s/m^2) versus the contralateral eye (Fig. 5). This implicates Kir4.1 in the STR and PhNR generation, likely through Müller cell action.

We did not always observe that the antibodies suppressed the ERG. We evaluated 10 such eyes by IHC, injected with Kir4.1-Ab:carrier or with Kir2.1-Ab:carrier and found that 8 showed no labeling or only diffuse and nonspecific tissue immunostaining, inconsistent with cellular delivery. This provides a control for associating the functional effect with antibody cellular binding.

Discussion

The approach of applying antibodies in vivo evolved from our experience with melanoma associated retinopathy (MAR) patients who suffer autoimmune vision loss and who exhibit selective loss of dark-adapted ERG b-wave but not a-wave response. Intravitreal injection into nonhuman primate of IgG fraction that we extracted from MAR patient blood serum rapidly altered the ERG in a fashion characteristic of presumed BC dysfunction of MAR patients (39). The present Kir-Ab study extends this strategy to controlled experiments using purified antibodies to target functional antigens potentially involved in ERG generation. Our findings indicate a role for Kir2.1 in the rod and cone proximal retinal pathway activity responsible for the STR and PhNR.

Two major study findings are that Kir2.1 and Kir4.1 antibodies applied in vivo reduced the STR and PhNR proximal-retinal corneal-negative ERG potentials and that the Kir2.1-Ab, which labeled BC synaptic terminals, reduced the Ba^{2+}-sensitive K^+ current in BC cell patch-clamp recordings. The ERG results support previous studies that used potassium electrodes and intraretinal depth recordings to demonstrate a role for Ba^{2+}-sensitive K^+ channels in generating the STR (7) and proximal retina cone pathway ERG potentials (8). Those approaches,
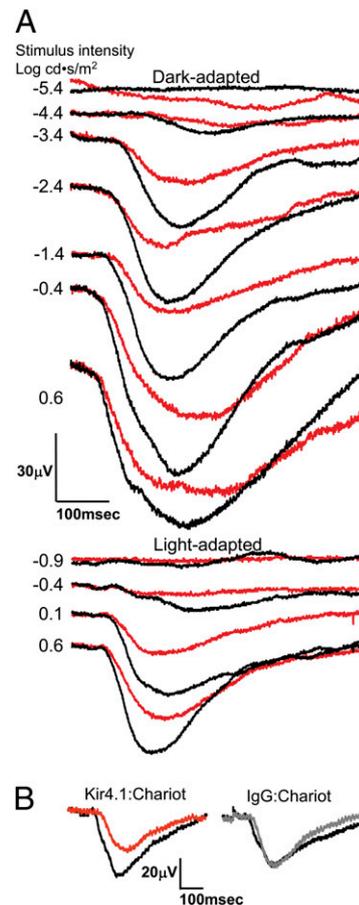
Fig. 5. In vivo intravitreal application of Kir4.1-Ab:carrier reduces STR and PhNR electronegative ERG potentials in RCS rat. (*A*) STR and PhNR were diminished in the eye of a 15-wk-old rat injected with Kir4.1-Ab:carrier (red) relative to the contralateral IgG:carrier control eye (black). (*B*) Light-adapted ERG responses (stimulus intensity 0.6 log cd-s/m^2) before (black) and 2 h after injection in a representative RCS rat at 14 wk of age. One eye was injected with Kir4.1-Ab:carrier (red) and the contralateral control eye with rabbit IgG:carrier (gray). PhNR amplitudes were decreased by $29 \pm 5\%$ ($n = 3$) compared with the same eye baseline, whereas no change in PhNR amplitude was seen in the contralateral control eyes.

however, cannot localize the channels to specific cell types nor evaluate contributions from specific Kir subtypes. A more recent study of the Kir4.1 knockout mouse demonstrated that these channels contribute to the ERG slow-PIII from the distal retina (10). Our findings using subtype-specific antibodies indicate that Kir2.1 activity is required to produce the STR and PhNR. This augments the ERG models of Frishman et al. (7, 8) and Kofuji and Newman (10–12) by placing strongly inward rectifying Ba^{2+}-sensitive Kir2.1 channels on rod and cone BC termini where they would subserve K^+ reuptake. In providing a sink for extracellular potassium concentration $[K^+]_o$, these channels may contribute directly to currents generating the ERG potentials. Alternatively, their ERG effect could be indirect, through a critical role of Kir2.1 in BC cell synaptic output leading to amacrine and/or ganglion cell activity, which contributes to the STR and PhNR in RCS rat (23, 24) and other species (20–22, 40).

Whole-cell voltage clamp recordings while dialyzing with Kir2.1-Ab through the recording pipette provided direct evidence that the antibody suppresses Kir2.1 current. Cone BC currents were suppressed consistently, whereas rod BCs exhibited two behaviors: some demonstrated considerable current suppression whereas others were minimally affected, raising the possibility of rod BC subpopulations that differ in Kir2.1 channel expression.

In considering a molecular mechanism of antibody action on channel function, one notes that the Kir2.1-Ab epitope lies on the C-terminal domain, which includes the PDZ-binding motif important for protein–protein interactions. Channel interaction with the cytoskeleton is regulated through a PSD-95 complex via a type-I PDZ binding motif (41, 42). The interaction with actin cytoskeleton through filamin-A may regulate location of the channel at the cell surface as well as the oligomerization state and stability. Cells that lack filamin-A have reduced whole-cell Kir2.1 currents, but filamin-A has no significant effect on single channel amplitude or open probability, suggesting a reduced number of functional channels in the cell membrane (42). We noted that Kir 2.1-Ab application in vivo reduced the STR and PhNR amplitudes maximally only by about half, which suggests that antibody attachment near the C terminus PDZ binding motif may similarly interrupt channel binding to cytoskeleton and reduce the number of functional channels. Kir2.1 crystal structure indicates that the 57 amino acids at the C terminus are highly mobile and require binding with some other domain to gain structural rigidity (43). Attachment of Kir2.1-Ab would interfere with such binding and interrupt normal channel function.

Antibodies were delivered in vivo with a readily available system that combines a cargo protein with the Pep-1 carrier peptide. Viruses and some higher organisms, including *Drosophila*, use specific peptide sequences such as the HIV-1 TAT sequence to convey proteins across biological membranes and into cells (44). Synthetic peptides have also been used for transfection in vitro and in vivo (45–47). However, these methods require labor-intensive fusion protein expression to combine the carrier peptide and cargo protein (44, 47), which the Pep-1 carrier bypasses. Pep-1 has been used successfully for in vitro delivery of antibodies and enzymes to several cell types such as osteoblasts (48) and human breast carcinoma (49), as well as for in vivo delivery such as to respiratory epithelium (50), dermal cells (51), and retinal cells (52). The results presented here indicate use of this strategy to probe function in vivo.

Methods

Animals. Pigmented dystrophic (p^+/Lav) and congenic nondystrophic (rdy^+p^+/Lav) RCS rats were used at 8–15 wk of age. Experiments were conducted in accordance with the ARVO Statement for the Use of Animals in Ophthalmic and Vision Research, and protocols were approved by the Animal Care and Use Committee of the National Eye Institute of National Institutes of Health.

Intravitreal Injections. We used a rabbit polyclonal Kir2.1-Ab against the C terminus peptide sequence NGVPESTSTDTPPDIDLHN corresponding to amino acid residues 392–410 of human Kir2.1 and Kir4.1-Ab against residues 356–375 in rat (Alomone Labs). Kir-Ab, 4 µg/µL, was mixed at 1:1 volume ratio with the protein carrier "Chariot" (Active Motif), corresponding to Pep-1 (46). Rats were dark-adapted overnight and then anesthetized (i.p. 80 mg/kg ketamine and 4 mg/kg xylazine). Following topical ocular anesthesia with 0.5% proparacaine, 5 µL of Kir-Ab:carrier was injected into the vitreous under dim red light using a microsyringe and 30-guage needle (Hamilton) through the temporal sclera 2 mm posterior to the limbus. The contralateral eye was injected with 5 µL rabbit IgG:carrier (Zymed Laboratories) as control. Rats were maintained in darkness until ERGs were recorded 1–2 h after injections.

Electroretinogram. ERGs were recorded as described previously (53). Dark-adapted STR and light-adapted PhNR amplitudes were measured from the baseline to the response trough, and b-wave amplitudes were measured from the baseline or from the a-wave trough if present. ERG values are given as mean ± SE.

Immunohistochemistry. IHC was performed in two ways: by conventional application of antibodies to postmortem fixed and sectioned tissue (24) or by in vivo intravitreal application of the Kir-Ab:carrier complex, after which the ERG generally was recorded, and rats were euthanized and enucleated. Eyes were processed by standard methods (24) except that if Kir-Ab had already been administered in vivo, it was not applied to the sections postmortem. In either case, antibodies for double labeling were applied postmortem to fixed sections.

Primary antibodies were polyclonal rabbit anti-human Kir2.1-Ab and Kir4.1-Ab (1:50 dilution; Alomone Labs), monoclonal mouse anti-human protein kinase C alpha (PKCα-Ab 1:200; Santa Cruz Biotechnology) to label rod BCs (54), monoclonal mouse anti-human protein kinase C beta (PKCβ-Ab, 1:200; Santa Cruz Biotechnology) to label cone BCs (33), polyclonal guinea-pig anti-rat vesicular glutamate transporter 1 (VGLUT1-Ab, 1:5,000; Chemicon) to label rod and cone BCs (55), polyclonal goat anti-human synapsin Ia/b-Ab (1:50; Santa Cruz Biotechnology) and IIa-Ab (1:100; Santa Cruz Biotechnology) as amacrine cell markers that label phosphoproteins of conventional synapses but not ribbon-containing terminals (35), and polyclonal GFAP-Ab (Sigma, 1:200) as Müller cell marker. Secondary antibodies were AlexaFluor 568 and AlexaFluor 488 (1:400; Invitrogen) and AlexaFluor 633 (1:300; Invitrogen). DNA binding fluorophore DAPI (4′,6-diamidino-2-phenyl-indole, dihydrochloride) (1 µg/mL; Invitrogen) was used to label cell nuclei.

Whole-Cell Recordings from Bipolar Cells in Retinal Slice. Whole-cell recordings from rod BCs and cone BCs were performed as described previously (56) with pipettes (8–10 MΩ) containing 110 mM KCl, 10 mM hepes, 10 mM glutamic acid, 10 mM EGTA, 10 mM NaPhosphocreatine, 4 mM MgATP, 0.4 mM NaGTP, and 0.02 mM Alexa 488 hydrazide. Retinal slices were placed into a recording chamber and continually superfused with artificial CSF (ACSF) containing (in mM): 119 NaCl, 26 $NaHCO_3$, 10 glucose, 1.25 NaH_2PO_4, 2.5 KCl, 2.5 $CaCl_2$, 1.5 $MgCl_2$, 4 NaLactate, and 2 NaPyruvate and bubbled with 95% O_2/5% CO_2 to maintain pH 7.4. Kir2.1-Ab or rabbit IgG (32 ng/µL) were added to this solution to explore the effect. A 10- to 15-min postbreak in dialysis period was allowed before measuring current amplitudes. Cells were identified morphologically post hoc using two-photon microscopy (810 nm; Zeiss). BC access resistance ranged from 30 to 60 MΩ and was left uncompensated and monitored online. Cells were used for analysis if holding currents were ≤50 pA (at −60 mV) and stable (Δihold <10 pA) throughout recordings. Cadmium (100 µM) and tetrodotoxin (1 µM) were used to block voltage-gated calcium and sodium channels, respectively. Currents were elicited at 17-s intervals and recorded (Axopatch 1D amplifier; Axon Instruments) with 5-kHz low-pass filtering. Data are presented as mean ± SD. Illustrated traces are averages of three to six responses.

1. Kofuji P, Newman EA (2004) Potassium buffering in the central nervous system. *Neuroscience* 129:1045–1056.

2. Doupnik CA, Davidson N, Lester HA (1995) The inward rectifier potassium channel family. *Curr Opin Neurobiol* 5:268–277.

3. Nichols CG, Lopatin AN (1997) Inward rectifier potassium channels. *Annu Rev Physiol* 59:171–191.

4. Ishii M, et al. (1997) Expression and clustered distribution of an inwardly rectifying potassium channel, KAB-2/Kir4.1, on mammalian retinal Müller cell membrane: Their regulation by insulin and laminin signals. *J Neurosci* 17:7725–7735.

5. Brew H, Gray PT, Mobbs P, Attwell D (1986) Endfeet of retinal glial cells have higher densities of ion channels that mediate K+ buffering. *Nature* 324:466–468.

6. Nagelhus EA, et al. (1999) Immunogold evidence suggests that coupling of K+ siphoning and water transport in rat retinal Müller cells is mediated by a coenrichment of Kir4.1 and AQP4 in specific membrane domains. *Glia* 26:47–54.

7. Frishman LJ, Steinberg RH (1989) Light-evoked increases in [K+]o in proximal portion of the dark-adapted cat retina. *J Neurophysiol* 61:1233–1243.

8. Frishman LJ, Yamamoto F, Bogucka J, Steinberg RH (1992) Light-evoked changes in [K+]o in proximal portion of light-adapted cat retina. *J Neurophysiol* 67:1201–1212.

9. Newman EA (1987) Regulation of potassium levels by Müller cells in the vertebrate retina. *Can J Physiol Pharmacol* 65:1028–1032.

10. Kofuji P, et al. (2000) Genetic inactivation of an inwardly rectifying potassium channel (Kir4.1 subunit) in mice: Phenotypic impact in retina. *J Neurosci* 20:5733–5740.

11. Newman E, Reichenbach A (1996) The Müller cell: A functional element of the retina. *Trends Neurosci* 19:307–312.

12. Newman EA, Frambach DA, Odette LL (1984) Control of extracellular potassium levels by retinal glial cell K+ siphoning. *Science* 225:1174–1175.

13. Tian M, Chen L, Xie JX, Yang XL, Zhao JW (2003) Expression patterns of inwardly rectifying potassium channel subunits in rat retina. *Neurosci Lett* 345:9–12.

14. Kubo Y, Baldwin TJ, Jan YN, Jan LY (1993) Primary structure and functional expression of a mouse inward rectifier potassium channel. *Nature* 362:127–133.

15. Morishige K, et al. (1993) Molecular cloning, functional expression and localization of an inward rectifier potassium channel in the mouse brain. *FEBS Lett* 336:375–380.

16. Prüss H, Derst C, Lommel R, Veh RW (2005) Differential distribution of individual subunits of strongly inwardly rectifying potassium channels (Kir2 family) in rat brain. *Brain Res Mol Brain Res* 139:63–79.

17. Iandiev I, et al. (2006) Differential regulation of Kir4.1 and Kir2.1 expression in the ischemic rat retina. *Neurosci Lett* 396:97–101.

18. Kofuji P, et al. (2002) Kir potassium channel subunit expression in retinal glial cells: Implications for spatial potassium buffering. *Glia* 39:292–303.

19. Chen L, Yu YC, Zhao JW, Yang XL (2004) Inwardly rectifying potassium channels in rat retinal ganglion cells. *Eur J Neurosci* 20:956–964.

20. Frishman LJ, Sieving PA, Steinberg RH (1988) Contributions to the electroretinogram of currents originating in proximal retina. *Vis Neurosci* 1:307–315.

21. Sieving PA, Frishman LJ, Steinberg RH (1986) Scotopic threshold response of proximal retina in cat. *J Neurophysiol* 56:1049–1061.

22. Viswanathan S, Frishman LJ, Robson JG, Harwerth RS, Smith EL, 3rd (1999) The photopic negative response of the macaque electroretinogram: Reduction by experimental glaucoma. *Invest Ophthalmol Vis Sci* 40:1124–1136.

23. Bush RA, Hawks KW, Sieving PA (1995) Preservation of inner retinal responses in the aged Royal College of Surgeons rat. Evidence against glutamate excitotoxicity in photoreceptor degeneration. *Invest Ophthalmol Vis Sci* 36:2054–2062.

24. Machida S, Raz-Prag D, Fariss RN, Sieving PA, Bush RA (2008) Photopic ERG negative response from amacrine cell signaling in RCS rat retinal degeneration. *Invest Ophthalmol Vis Sci* 49:442–452.

25. D'Cruz PM, et al. (2000) Mutation of the receptor tyrosine kinase gene Mertk in the retinal dystrophic RCS rat. *Hum Mol Genet* 9:645–651.

26. Dowling JE, Sidman RL (1962) Inherited retinal dystrophy in the rat. *J Cell Biol* 14:73–109.

27. Herron WL, Riegel BW, Myers OE, Rubin ML (1969) Retinal dystrophy in the rat—a pigment epithelial disease. *Invest Ophthalmol* 8:595–604.

28. Jones BW, et al. (2003) Retinal remodeling triggered by photoreceptor degenerations. *J Comp Neurol* 464:1–16.

29. Villegas-Pérez MP, Lawrence JM, Vidal-Sanz M, Lavail MM, Lund RD (1998) Ganglion cell loss in RCS rat retina: A result of compression of axons by contracting intraretinal vessels linked to the pigment epithelium. *J Comp Neurol* 392:58–77.

30. Ma YP, Cui J, Hu HJ, Pan ZH (2003) Mammalian retinal bipolar cells express inwardly rectifying K+ currents (IKir) with a different distribution than that of Ih. *J Neurophysiol* 90:3479–3489.

31. Lei B, Perlman I (1999) The contributions of voltage- and time-dependent potassium conductances to the electroretinogram in rabbits. *Vis Neurosci* 16:743–754.

32. Solessio E, Linn DM, Perlman I, Lasater EM (2000) Characterization with barium of potassium currents in turtle retinal Müller cells. *J Neurophysiol* 83:418–430.

33. Kosaka J, Suzuki A, Morii E, Nomura S (1998) Differential localization and expression of alpha and beta isoenzymes of protein kinase C in the rat retina. *J Neurosci Res* 54:655–663.

34. Osborne NN, Broyden NJ, Barnett NL, Morris NJ (1991) Protein kinase C (alpha and beta) immunoreactivity in rabbit and rat retina: Effect of phorbol esters and transmitter agonists on immunoreactivity and the translocation of the enzyme from cytosolic to membrane compartments. *J Neurochem* 57:594–604.

35. Mandell JW, et al. (1990) Synapsins in the vertebrate retina: Absence from ribbon synapses and heterogeneous distribution among conventional synapses. *Neuron* 5:19–33.

36. Grünert U, Martin PR (1991) Rod bipolar cells in the macaque monkey retina: Immunoreactivity and connectivity. *J Neurosci* 11:2742–2758.

37. Mattig WU, Hanitzsch R (1993) The ERG and light-induced extracellular potassium changes in the isolated superfused RCS rat retina. *Clin Vis Sci* 8:513–518.

38. Newman EA (1993) Inward-rectifying potassium channels in retinal glial (Müller) cells. *J Neurosci* 13:3333–3345.

39. Lei B, Bush RA, Milam AH, Sieving PA (2000) Human melanoma-associated retinopathy (MAR) antibodies alter the retinal ON-response of the monkey ERG in vivo. *Invest Ophthalmol Vis Sci* 41:262–266.

40. Saszik SM, Robson JG, Frishman LJ (2002) The scotopic threshold response of the dark-adapted electroretinogram of the mouse. *J Physiol* 543:899–916.

41. Cohen NA, Brenman JE, Snyder SH, Bredt DS (1996) Binding of the inward rectifier K+ channel Kir 2.3 to PSD-95 is regulated by protein kinase A phosphorylation. *Neuron* 17:759–767.

42. Sampson LJ, Leyland ML, Dart C (2003) Direct interaction between the actin-binding protein filamin-A and the inwardly rectifying potassium channel, Kir2.1. *J Biol Chem* 278:41988–41997.

43. Pegan S, et al. (2005) Cytoplasmic domain structures of Kir2.1 and Kir3.1 show sites for modulating gating and rectification. *Nat Neurosci* 8:279–287.

44. Fawell S, et al. (1994) Tat-mediated delivery of heterologous proteins into cells. *Proc Natl Acad Sci USA* 91:664–668.

45. Johnson LN, Cashman SM, Kumar-Singh R (2008) Cell-penetrating peptide for enhanced delivery of nucleic acids and drugs to ocular tissues including retina and cornea. *Mol Ther* 16:107–114.

46. Morris MC, Depollier J, Mery J, Heitz F, Divita G (2001) A peptide carrier for the delivery of biologically active proteins into mammalian cells. *Nat Biotechnol* 19:1173–1176.

47. Pooga M, et al. (1998) Cell penetrating PNA constructs regulate galanin receptor levels and modify pain transmission in vivo. *Nat Biotechnol* 16:857–861.

48. Selim AA, et al. (2003) Anti-osteoactivin antibody inhibits osteoblast differentiation and function in vitro. *Crit Rev Eukaryot Gene Expr* 13:265–275.

49. Remacle AG, et al. (2005) The transmembrane domain is essential for the microtubular trafficking of membrane type-1 matrix metalloproteinase (MT1-MMP). *J Cell Sci* 118:4975–4984.

50. Aoshiba K, Yokohori N, Nagai A (2003) Alveolar wall apoptosis causes lung destruction and emphysematous changes. *Am J Respir Cell Mol Biol* 28:555–562.

51. Choi SH, et al. (2006) Human PEP-1-ribosomal protein S3 protects against UV-induced skin cell death. *FEBS Lett* 580:6755–6762.

52. Wang MH, Frishman LJ, Otteson DC (2009) Intracellular delivery of proteins into mouse Müller glia cells in vitro and in vivo using Pep-1 transfection reagent. *J Neurosci Methods* 177:403–419.

53. Raz-Prag D, Zeng Y, Sieving PA, Bush RA (2009) Photoreceptor protection by adeno-associated virus-mediated LEDGF expression in the RCS rat model of retinal degeneration: Probing the mechanism. *Invest Ophthalmol Vis Sci* 50:3897–3906.

54. Greferath U, Grünert U, Wässle H (1990) Rod bipolar cells in the mammalian retina show protein kinase C-like immunoreactivity. *J Comp Neurol* 301:433–442.

55. Johnson J, et al. (2003) Vesicular neurotransmitter transporter expression in developing postnatal rodent retina: GABA and glycine precede glutamate. *J Neurosci* 23:518–529.

56. Singer JH, Diamond JS (2003) Sustained Ca2+ entry elicits transient postsynaptic currents at a retinal ribbon synapse. *J Neurosci* 23:10923–10933.